Absolute measurements of total target strength from reverberation in a cavity

David A. Demer
Southwest Fisheries Science Center, 8604 La Jolla Shores Drive, La Jolla, California 92037

Stephane G. Conti
Southwest Fisheries Science Center, 8604 La Jolla Shores Drive, La Jolla, California 92037, Universite Pierre et Marie Curie - Paris VI, 4 Place Jussieu, 75005 Paris, France, and Laboratoire Ondes et Acoustique, 10 Rue Vauquelin, 75005 Paris, France

Julien De Rosny
Marine Physical Laboratory, SIO/UCSD, 9500 Gilman Drive, La Jolla, California 92093-0205

Philippe Roux
Laboratoire Ondes et Acoustique, 10 Rue Vauquelin, 75005 Paris, France

(Received 30 October 2001; revised 9 October 2002; accepted 4 December 2002)

A new method was developed to acoustically measure the density and total scattering cross-section (σ_t) or total target strength [$\mathrm{TTS}=10\log_{10}(\sigma_t/4\pi)$] of objects in motion in a highly reflective cavity [J. De Rosny and P. Roux, J. Acoust. Soc. Am. **109**, 2587–2597 (2001)]. From an ensemble of pulse-echo recordings, the average contribution of the scatterer(s) to the reverberation within the cavity provides a measurement of the scattering mean free path. The latter was shown through theory and experiment to be proportional to the volume of the cavity and inversely proportional the product of the mean σ_t and number of scatterers. Here, the TTS measurement uncertainty is characterized using standard metal spheres as references. Theoretical TTS was calculated for multiple copper and tungsten carbide standard spheres (Cu: 60.0 30.05 and 23 mm and WC: 38.1 and 33.4 mm diameters, respectively), using well-described theory for scattering from elastic spheres and the optical theorem. Measurements of TTS were made over a wide bandwidth (30–120 kHz) and compared to their theoretical values. Measurements were made in a corrugated, cylindrical, galvanized-steel tank with 25 or 50 l of fresh water at a temperature of 21 ± 1 °C. The results indicate the method can provide TTS measurements that are accurate to at least 0.4 dB with an average precision of ±0.7 dB (95% confidence interval). Discussed are the requisite cavity volumes and signal-to-noise ratios for quality measurements of TTS, tank volume, and/or numerical abundance of mobile targets. Also discussed are multiple potential applications of this technique in bioacoustical oceanography. [DOI: 10.1121/1.1542648]

PACS numbers: 43.30.Xm, 43.30.Gv, 43.30.Sf, 43.80.Ev [DLB]

I. INTRODUCTION

Recently, a new method was invented to measure the number (n_s) of moving scatterers in a highly reverberant cavity (De Rosny, 2000). The theory was applied to acoustically counting fish in tanks (De Rosny and Roux, 2001). The method can also be used to estimate the volume of a cavity (v), or the total scattering cross-section (σ_t) of the scatterer(s) therein. Moreover, estimates of sound speed (c) and absorption cross-sections are also theoretically possible. Here, the accuracy and precision of the method for measuring σ_t is investigated using standard metal spheres as references.

In the new method, numerous pulses of sound ($i\in[1,N]$) are transmitted into a cavity having a static shape and volume. If the cavity hosts one or more mobile sound scatterers, the reverberation over time (t) resulting from the ith shot [$h^i(t)$] is comprised of echoes from (1) the motionless boundaries and (2) the moving object(s). For a single transmission, the two parts cannot be delineated. However, if the positions of the emitter and the receiver are fixed, the reverberation from the boundaries is coherent between records, while scatter from the moving objects is incoherent. By averaging N pulse-echo recordings (noted $\langle\,\rangle$), the parts of the signal due to the mobile scatterers are attenuated due to destructive interference, while that from the boundaries is reinforced. Following De Rosny and Roux (2001), the scattering mean free path (l_s, which characterizes σ_t, n_s, v, and c) can be estimated from the slope of the coherent sound intensity ($I_c=\langle h^i(t)\rangle^2$), divided by the incoherent intensity ($I_t=\langle h^i(t)^2\rangle$):

$$\frac{\langle h^i(t)\rangle^2}{\langle h^i(t)^2\rangle}\approx e^{-ct/l_s}. \tag{1}$$

This approximation does not depend on absorption in the medium nor on attenuation at the cavity interfaces, and is valid at time t when cavity echoes are present (De Rosny and Roux, 2001). It does require that the cavity conditions and boundaries are constant throughout the N recordings of $h^i(t)$.

TABLE I. Physical properties of copper (Cu) and tungsten carbide (WC) spheres that are relevant to their scattering cross-sections. Values for the material density (ρ_1) and longitudinal and transverse sound speeds (c_1 and c_2, respectively) for Cu and WC are from Foote and MacLennan (1984) and MacLennan and Dunn (1984), respectively.

	Cu	WC
ρ_1 (kg/m^3)	8947	14900
c_1 (m/s)	4760	6853
c_2 (m/s)	2288.5	4171

In practice, the cavity conditions are seldom static. For example, during the acquisition of N pulse-echo recordings, c may change appreciably due to temperature fluctuations. Therefore, l_s is better estimated from the slope ($d\ln(S)/dt$) of the average correlation of successive backscattered signals (De Rosny and Roux, 2001):

$$S(t)=\left(\frac{\langle h^i(t)h^{i+1}(t)\rangle}{\langle h^i(t)^2\rangle}\right)\approx e^{-ct/l_s} \tag{2}$$

$$\frac{d\ln(S)}{dt}\approx\frac{-cn_s\sigma_t}{\nu}. \tag{3}$$

The derivation of $S(t)$ is detailed in De Rosny and Roux (2001), and is therefore not repeated here. They showed that this estimator is totally dependent on the number of emitter-receiver positions in the average, the bandwidth of the emitted signal, and the ergodicity of the cavity (i.e., constancy of cavity conditions and boundaries). That is, the estimator is most robust for measurements that are averaged over multiple variations of the system (i.e., cavity+emitter +receiver). A practical approach to obtaining multiple system geometries is to use an omnidirectional emitter and receiver and a chirp transmission.

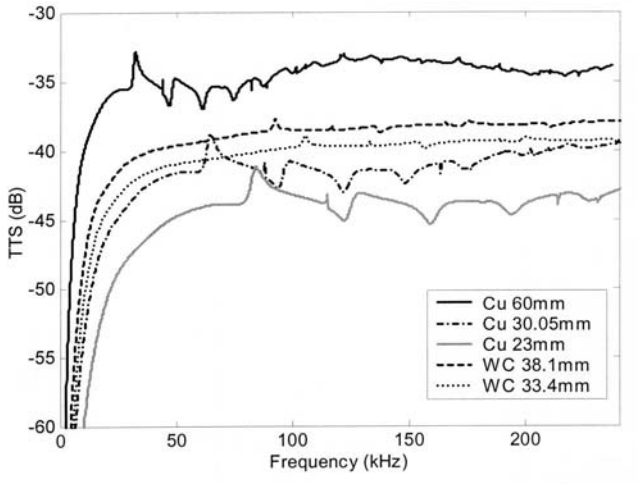

FIG. 1. Theoretical total target strengths [$\mathrm{TTS}=10\log_{10}(\sigma_t/4\pi)$] for standard spheres: electrolytic-grade copper (Cu) spheres (60-, 30.05-, 23-, and 13-mm diameters) and tungsten carbide (WC) with 6% cobalt binder (38.1- and 33.4-mm diameter). These curves were generated using the equations detailed in the Appendix, material properties from Table I, sound speed in water $c_3=1488$ m/s, and water density $\rho_3=1030$ kg/m^3. The spheres were suspended from loops of monofilament line affixed with epoxy into a small bore.

To determine the efficacy of this measurement technique, precision metal spheres were used as references. The theory of scattering from elastic spheres is well described (e.g., Faran, 1951; Hickling, 1962, 1964). MacLennan (1981) tabulated these equations for computing backscattering cross-sections of metal spheres with material density (ρ_1) and longitudinal and transverse sound speeds (c_1 and c_2, respectively). These equations are extended here, in the Appendix, to derive total scattering cross-sections (σ_t). Foote and MacLennan (1984) and MacLennan and Dunn (1984) provided accurate values of ρ_1, c_1, and c_2 for

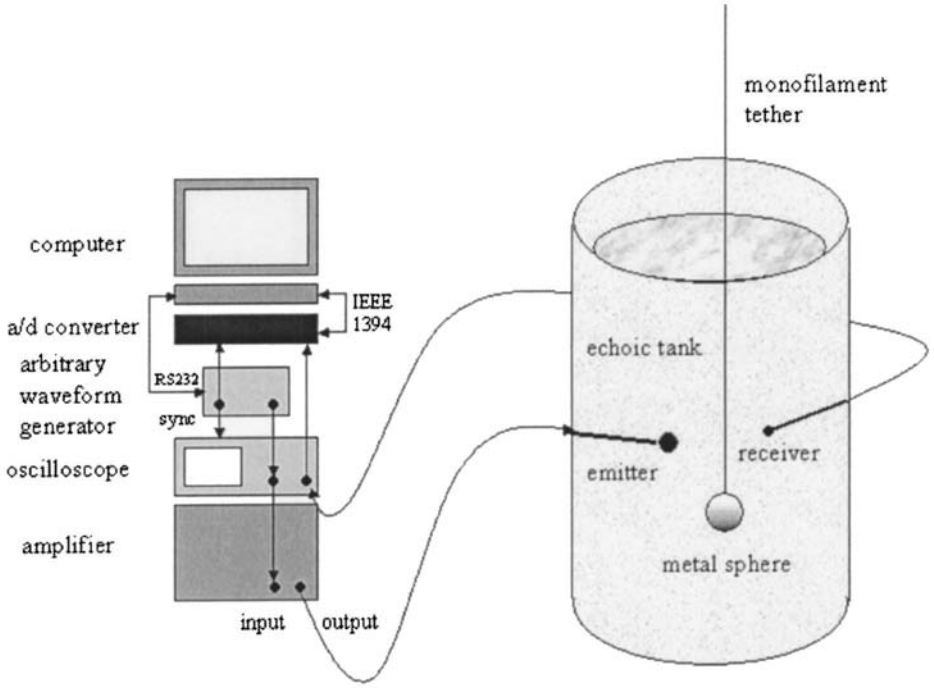

FIG. 2. Experimental apparatus. A corrugated, cylindrical, galvanized-steel tank was filled with fresh water. Chirp-pulses were created with an arbitrary waveform generator (Hewlett Packard 33120A), amplified by a broadband power amplifier (ENI 1140LA) and projected with an omnidirectional source (ITC 1042). Signals were received using an omnidirectional receiver (Reson 4013), digitized with a high-speed analog-to-digital converter (National Instruments Daqpad 6070E) and logged and processed on a laptop computer (Dell Inspiron 7500).

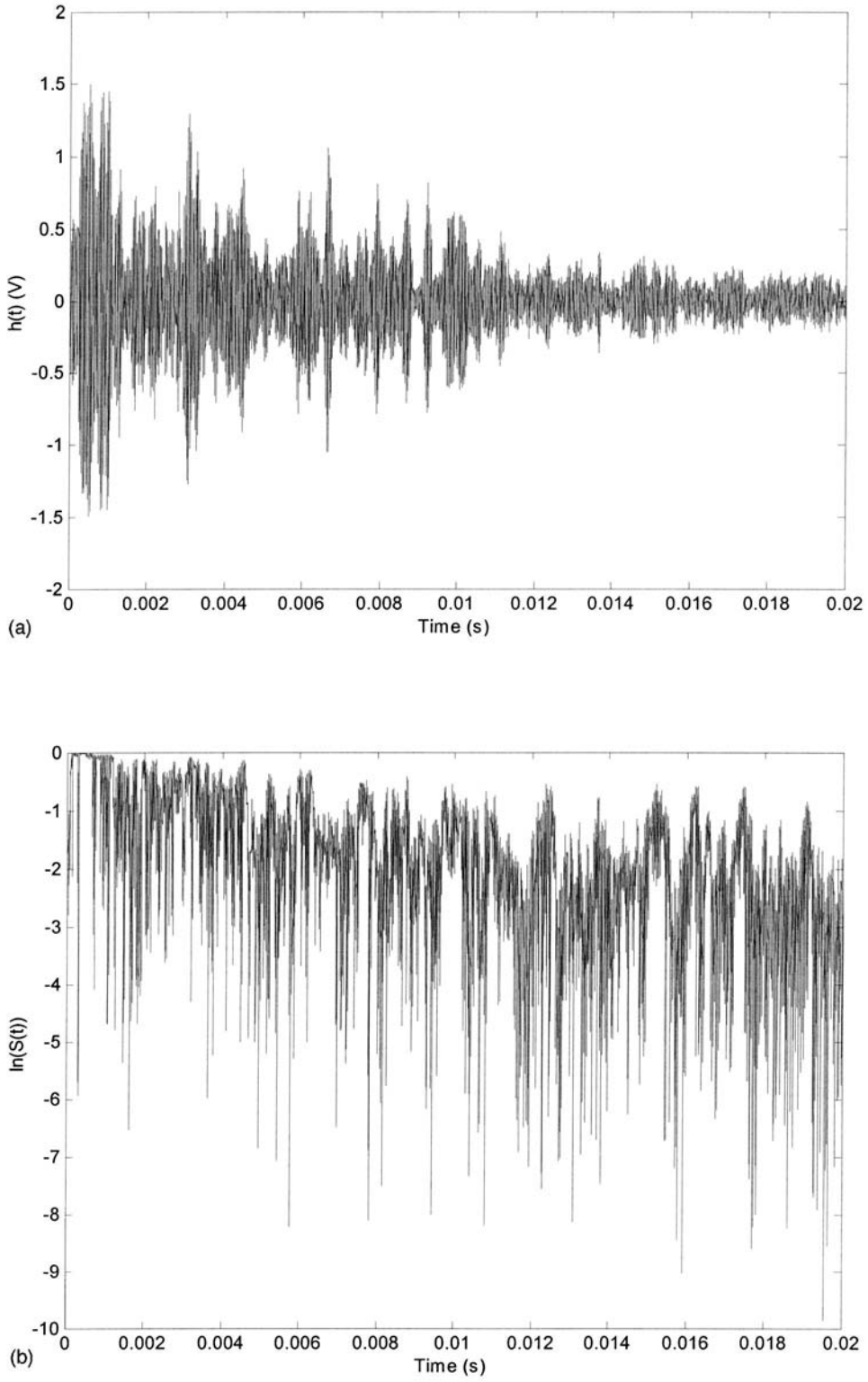

FIG. 3. Reverberation time-series $[h(t)]$ (a) and the natural logarithm of the estimator $S(t)$ (b) for a 60-mm-diam copper sphere (center frequency $=100$ kHz).

spheres made from copper (Cu) and tungsten carbide (WC) with 6% cobalt binder, respectively (Table I). Such spheres are routinely used as calibration references for scientific echosounders (e.g., Foote, 1982, 1990).

II. METHODS

Using the equations and material property values tabulated in the Appendix and Table I, respectively, theoretical σ_t were computed for five metal spheres (60, 30.05, and 23 mm Cu, and 38.1- and 33.4-mm-diam WC. The total target strength $[\mathrm{TTS}=10\log_{10}(\sigma_t/4\pi)]$ was also computed for each sphere (Fig. 1).

Measurements of TTS of metal spheres were made in August 2001 in the Advanced Survey Technologies Laboratory of the Southwest Fisheries Science Center. A corrugated, cylindrical, galvanized-steel tank, 54 cm in diameter and 67 cm tall was filled with 25 or 50 l of fresh water at a temperature $t_w=21\pm1$ °C (Fig. 2). Chirp-pulses of 500-μs duration,

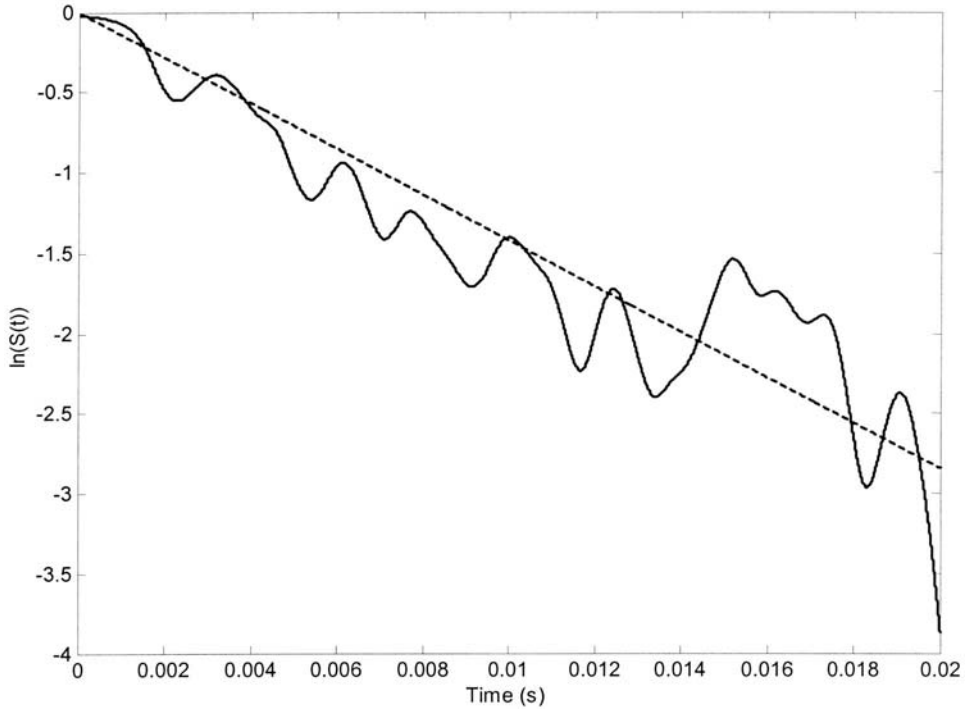

FIG. 4. The exponential decay of $S(t)$ was estimated for each 200-record ensemble by separately low-pass filtering the numerator and denominator of the function in the linear domain ($f_{\text{cutoff}} = 500$ Hz), transforming it to the logarithmic domain (—), and fitting a slope $[d \ln(S)/dt]$ in the least-squares sense, while requiring $2 \leqslant t \leqslant 15$ ms for the 50-l cavity and $2 \leqslant t \leqslant 10$ ms for the 25-l cavity, and $\ln(S) = 0$ at $t = 0$ (--). This example is from the 60-mm-diam copper sphere at a center frequency of 100 kHz.

2-Hz repetition rate, amplitudes of 400 or 170 $\text{mV}_{\text{p-p}}$, and center frequencies (f_c) from 30 to 50 kHz and 52 to 120 kHz, respectively, were created with an arbitrary waveform generator (Hewlett Packard 33120A). These 2-kHz bandwidth pulses were amplified 55 dB by a wide-bandwidth power amplifier (225 or 95.6 $\text{V}_{\text{p-p}}$; ENI 1140LA) and projected with a wide-bandwidth omnidirectional emitter (ITC 1042). The source was suspended 21.5 cm from the side of the tank and either 40 or 8 cm deep. Signals were received using a wide-bandwidth omnidirectional receiver (Reson 4013), placed 14 cm from the side of the tank and either 39.5 or 7.5 cm deep, depending on the water volume. The emitter and receiver were positioned towards the center of the tank so the observed sound pressure was not affected by the boundaries.

The precision metal spheres were placed in the tank one at a time. Continuously throughout the measurements, the spheres were laboriously moved by hand around the tank via the monofilament tether in a quasi-random three-dimensional motion. The speed of the manual motion was fast enough to

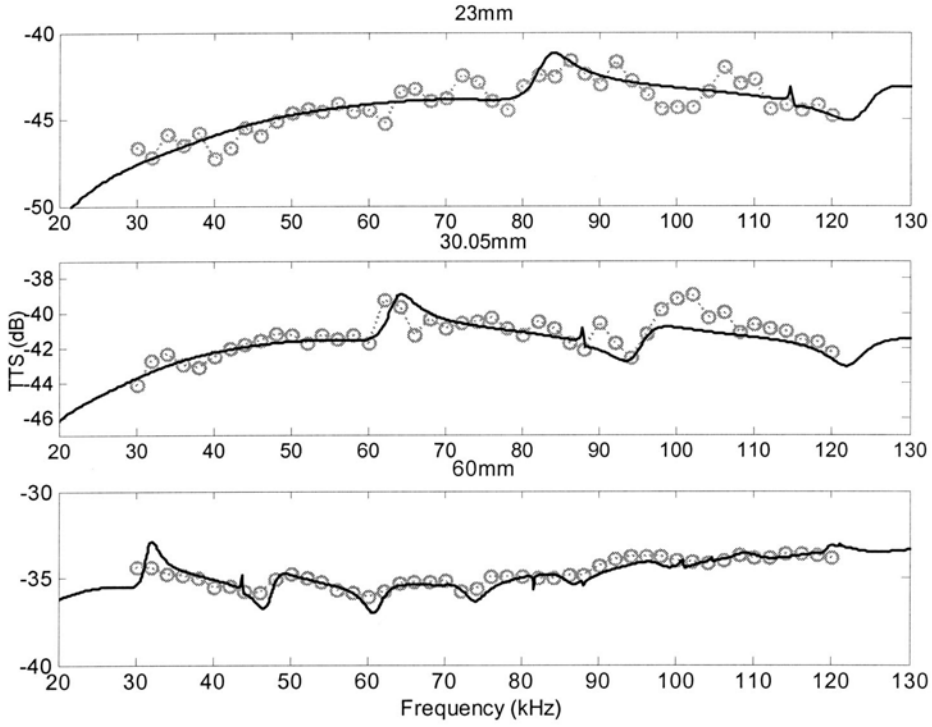

FIG. 5. Theoretical (−) and measured (-o-) TTS for 23-, 30.05-, and 60.0-mm-diam copper spheres. For the two smaller spheres, data were obtained in a single cavity, whereas the TTS measurements for the 60-mm-diam sphere were obtained with an average over three cavities (variations of receiver positions and tank volumes: 100 and 50 l). Differences between the measurements and theory are generally less than 1 dB.

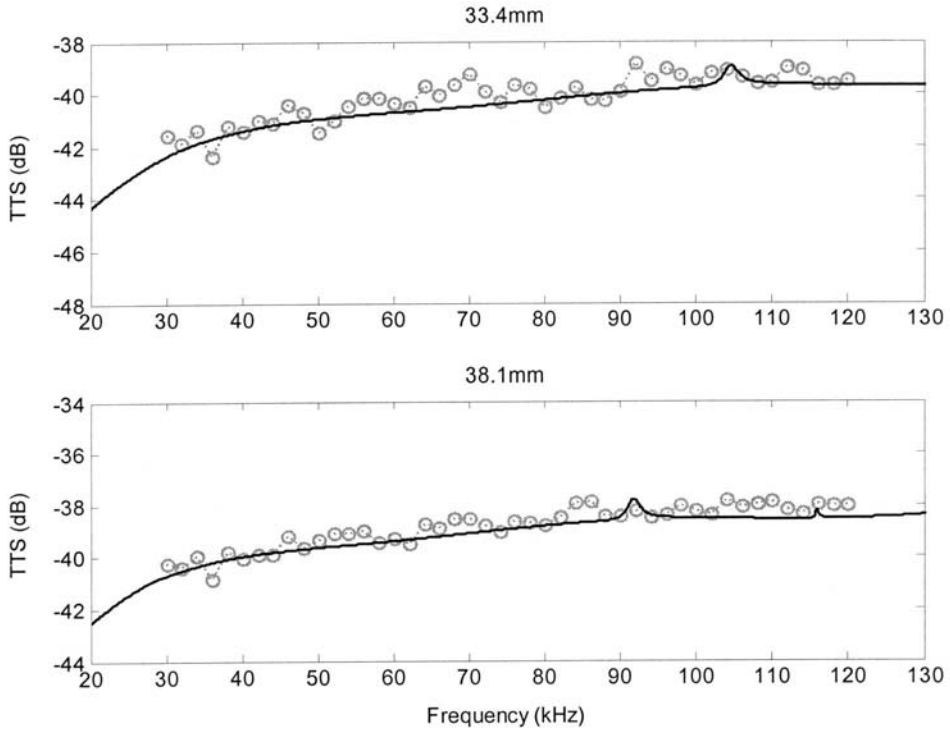

FIG. 6. Theoretical (−) and measured (-o-) TTS of 33.4- and 38.1-mm-diam tungsten carbide spheres (with 6% cobalt binder). Data were obtained for the 33.4-mm-diam sphere in a single cavity, whereas the TTS measurements for the 38.1-mm-diam sphere were obtained with an average over three cavities [variations of receiver positions and tank volumes (100 and 50 l)]. Again, differences between the measurements and theory are generally less than 1 dB.

maintain a very low correlation in reverberation between pings, yet slow enough that the water surface was not noticeably disturbed.

For each of 200 pings at each f_c, 32 ms of reverberation $[h^i(t)]$ were recorded using a 12-bit analog-to-digital converter (National Instruments Daqpad 6070E), sampling at 400 kHz (e.g., Fig. 3). The exponential decay of $S(t)$ was estimated for each 200-record ensemble by separately low-pass filtering the numerator and denominator of the function in the linear domain ($f_{\text{cutoff}}=500$ Hz), and fitting a slope $[d\ln(S)/dt]$ in the least-squares sense, while requiring $2\leqslant t \leqslant 15$ ms for the 50-l cavity and $2\leqslant t\leqslant 10$ ms for the 25-l cavity, and $\ln(S)=0$ at $t=0$ (Fig. 4). $S(t)$ was low-pass filtered before the ratio to average the nulls of the cavity. This procedure is useful for low frequencies, when a small number of modes are excited in the cavity. For higher frequencies, low-pass filtering $S(t)$ before or after the ratio provides the same results. From $d\ln(S)/dt$ an estimate of σ_t was made for each sphere and frequency:

$$\sigma_t \approx -\frac{\nu}{cn_s}\frac{d\ln(S)}{dt}. \tag{4}$$

Corresponding TTSs were then computed and compared to theory (Figs. 5 and 6). From the Appendix, theoretical values for σ_t (and TTS) can be equivalently computed by the discrete integration of the form function, an analytical integration of the Legendre polynomial, or by applying the optical theorem (Feenberg, 1932). All methods were tried, but for ease and speed of computations, the latter method was ultimately chosen.

To estimate the accuracy and precision of the method, the 60-mm-diam Cu and 38.1-mm-diam WC spheres were selected as references. For each of these two spheres, three estimates of TTS were obtained for each frequency. Mean values, standard deviations (sd), and 95% confidence intervals (± 2 sd) were computed for each frequency (Fig. 7).

III. RESULTS

The wide-bandwidth measurements of TTS for the Cu and WC spheres were compared to their theoretical counterparts (Figs. 5 and 6, respectively). For all five spheres, there is a remarkable agreement between the empirical and theoretical data–mean discrepancies are only a few tenths of a decibel and the dynamics of the form function track closely. In some cases (e.g., the 30.05-mm-diam Cu sphere circa 62 kHz), slight discrepancies between the theoretical and empirical null positions may be due to a mismatch between the selected and actual sound speeds in the water [1488 vs 1485 ± 3 m/s, respectively; calculating $c(t_w)$ as in Lubbers and Graaf (1998)], or in c_1 or c_2.

Averaging three measurements at each frequency, TTS measurements were plotted with their 95% confidence intervals and compared to theory for both the 60 mm Cu and 38.1 mm WC spheres (Fig. 7). For the 60 mm Cu sphere, the mean difference between the theoretical and experimental TTS for each frequency is 0.46 dB with a sd of 0.34 dB. For the 38.1 mm WC sphere, the mean difference is 0.40 dB, with a sd of 0.36 dB.

IV. CONCLUSION

The new technique based on multiple scattering can be used to measure the TTS of a single scatterer moving in an echoic cavity, over a wide bandwidth and with low uncertainty. This study shows that for two spheres of different materials and sizes, the mean difference between the experimental estimates of TTS and theory is 0.4 dB with an average precision of ± 0.7 dB (95% confidence interval). Al-

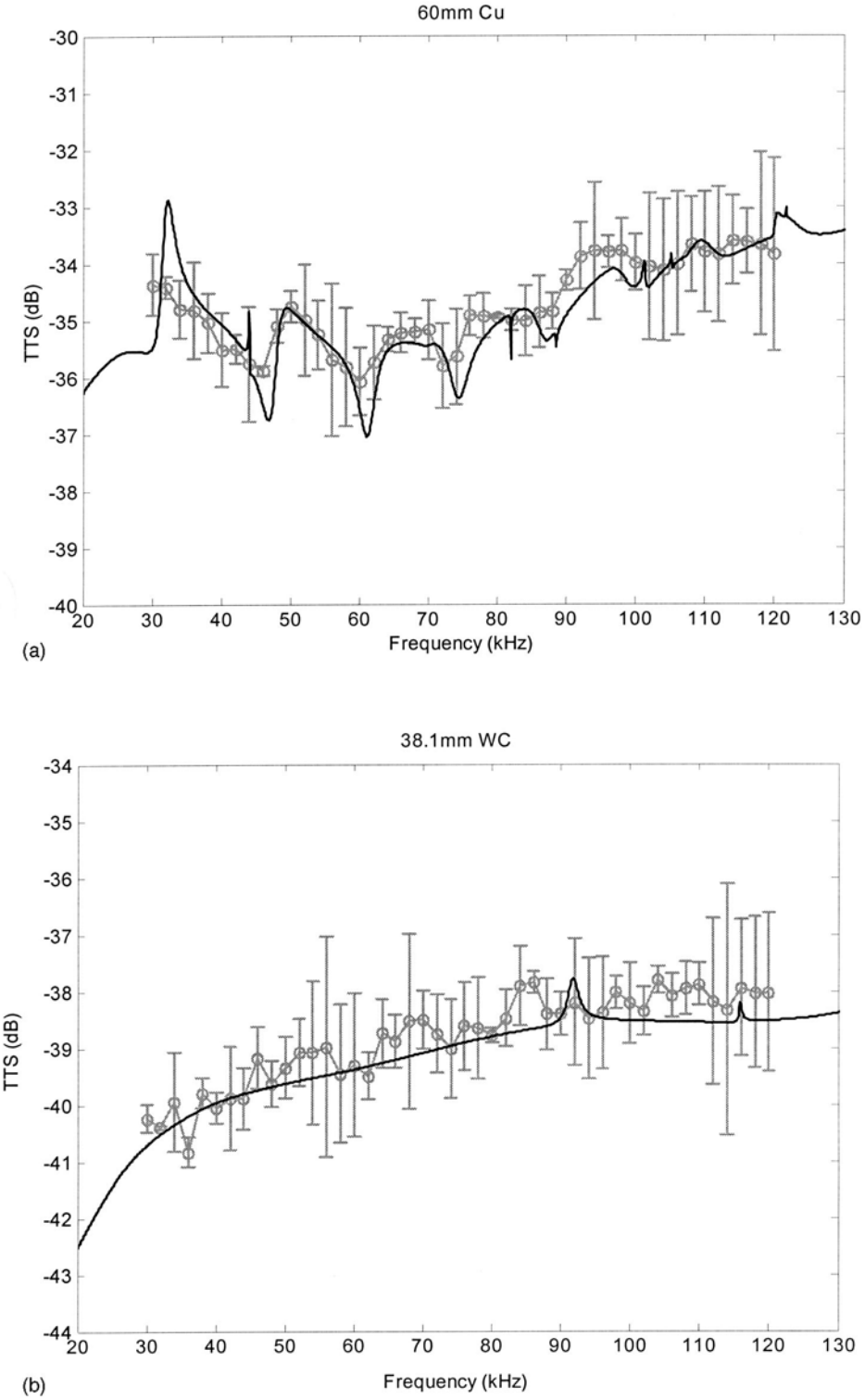

FIG. 7. TTS measurements (-o-) of the 60-mm-diam copper (a) and 38.1-mm-diam tungsten carbide spheres (b), and their 95% confidence intervals. The error bars (± 2 st. dev. $= \pm 0.67$ and ± 0.72 dB, respectively) generally encompass the theoretical TTS (—).

though this uncertainty is likely to be acceptable for most applications, there are some possibilities for improving upon these measurements.

Here, variables v and c were only estimated to within $\pm 0.5\%$ and 0.2%, respectively. The values of v and c could be more accurately estimated using traditional methods or by multi-dimensional application of the multi-scattering technique. That is, x-independent sets of measurements could be made and solved for x-unknown variables. The variance of the TTS measurements could be improved by a factor of $1/M$, by averaging M sets of σ_t measurements at each frequency. Moreover, the variance could be reduced by making physical changes to the cavity, its volume, and the positions of the emitter and receiver between measurement sets. Regarding the reference targets, there are also some minor uncertainties associated with the sizes, shapes, materials, densities, and c_1 or c_2 of the spheres (Foote and MacLennan, 1984).

It should also be mentioned that there are many requisite

considerations for making TTS measurements as good as the ones in this study. For example, to obtain a homogeneous sound field, a large number of modes must be excited in the cavity. Therefore, the characteristic size of the cavity, or smallest dimension, must be much greater than the wavelength ($\lambda = c/f$). As a guideline, $v \geqslant 100\lambda^3$ (e.g., $v \geqslant 12l$ at 30 kHz). Thus, the frequency range in these measurements (30 to 120 kHz) was rather limited by the frequency responses of the emitter and receiver. Additionally, v should not be too large compared to the total volume of the scatterers, and the reflectivity of the boundaries must be high, else the signal-to-noise ratio is insufficient. Many cavity materials were tested: fiberglass, high-density polyethylene, glass, and galvanized steel. Of these, the best reflectivity coefficients and thus the longest reverberation signals were obtained in the glass and galvanized steel tanks.

The TTSs of standard metal spheres were measured using the new multi-scattering method because the results could be confidently compared to primary standards. Although these measurements characterize the uncertainty in the multi-scattering method and constitute the first wide-bandwidth measurements of σ_t for metal spheres, other applications of the method are plentiful. De Rosny and Roux (2001) showed that the method could be used to accurately determine the number of fish in a tank. This could be useful in aquaculture. Of interest to the bioacoustical oceanographic community is the possibility for conveniently making wide-bandwidth measurements of total scattering cross-sections, resonant frequencies, and absorption cross-sections of oceanic sound scatterers. These data can be used to provide wide-bandwidth ''acoustical signatures'' for remotely identifying and classifying animals of a variety of species and sizes (Conti and Demer, submitted; and Demer and Conti, submitted).

Another interesting potential of this method is the characterization of σ_t as a function of animal size, shape, density, sound speed, and ambient pressure. Such data could be used for investigating both acoustical and biological properties of live animals and thus to improve the effectiveness of remote sensing tools such as echo-integration (e.g., Ehrenberg and Lytle, 1972), multiple-frequency target strength estimation and species delineation (Demer *et al.*, 1999), and bioacoustical absorption spectroscopy (e.g., Weston, 1967; Diachok *et al.*, 2001). Moreover, the data could provide much needed empirical validation of acoustical backscattering models (extended to σ_t) for a variety of fish (e.g., Love, 1977) and zooplankton (e.g., McGehee *et al.*, 1998; Demer and Conti, in press). While echo integration theory is based on backscattering, there are definable relationships (approximate if not analytically exact) between TTS and target strength for many scatterer types (morphologies, shapes, and orientation distributions), especially at low and high ka values.

ACKNOWLEDGMENTS

We are appreciative of William Kuperman, Director of Scripps Institution of Oceanography's Marine Physical Laboratory, and Rennie Holt, Director of the United States Antarctic Marine Living Resources Program, for co-sponsoring SC during his internship at the Southwest Fisheries Science Center. Thanks also to Charles Greenlaw, Ocean Sciences Group, BAE Systems; Andrew Brierley, Gatty Marine Laboratory, University of St. Andrews; and two anonymous reviewers for their helpful comments.

APPENDIX: THEORETICAL TOTAL SCATTERING CROSS-SECTION OF A SOLID ELASTIC SPHERE

The sound scatter from a solid elastic sphere in water was first computed by Faran (1951) and corrected by Hickling (1962, 1964). MacLennan (1981) tabulated these equations for computing the backscattering cross section of solid elastic spheres. The following is an extension of these equations, using Faran's symbols, to compute the total scattering cross-section.

In polar coordinates, for a plane wave of constant amplitude traveling in the z direction, the incident acoustic pressure at time t is

$$p_i(r,\theta,t) = p_0 \exp\{i(\omega t - k_3 r\cos\theta)\},$$

where k_3 is the wave number in the water and ω is the angular frequency. Interacting with a solid elastic sphere, the time-dependent scattered pressure is:

$$p_s(r,\theta,t) = p_{s0}(r,\theta)\exp(i\omega t),$$

where the forward- and backscattered pressures are defined at angles $\theta = 0$ and $\theta = \pi$, respectively. The scattered pressure can also be written as a sum of partial waves:

$$\begin{aligned} p_{s0}(r,\theta) &= -p_0 \sum_{n=0}^{\infty} (-i)^{n+1}(2n+1)\sin\eta_n \\ &\quad \times \exp(i\eta_n) h_n(k_3 r) P_n(\cos\theta) \\ &= -p_0 f(\theta, r), \end{aligned}$$

where $P_n(\cos\theta)$ is a Legendre polynomial, and $h_n(k_3 r)$ is the spherical Hankel function of the second kind, defined by

$$h_n(x) = j_n(x) - i n_n(x),$$

$$j_n(x) = J_{n+1/2}(x)\sqrt{\frac{\pi}{2x}}, \quad n_n(x) = N_{n+1/2}(x)\sqrt{\frac{\pi}{2x}},$$

where J and N are the Bessel functions of the first and second kind, respectively. The following equations determine η_n:

$$x_3 = k_3 a, \quad x_1 = \frac{x_3 c_3}{c_1}, \quad x_2 = \frac{x_3 c_3}{c_2},$$

$$A_2 = (n^2 + n - 2) j_n(x_2) + x_2^2 j_n''(x_2),$$

$$A_1 = 2n(n+1)[x_1 j_n'(x_1) - j_n(x_1)],$$

$$\alpha = 2\left(\frac{\rho_1}{\rho_3}\right)\left(\frac{c_2}{c_3}\right)^2, \quad \beta = \left(\frac{\rho_1}{\rho_3}\right)\left(\frac{c_1}{c_3}\right)^2 - \alpha,$$

$$\begin{aligned} B_2 &= A_2 x_1^2 [\beta j_n(x_1) - \alpha j_n''(x_1)] \\ &\quad - A_1 \alpha [j_n(x_2) - x_2 j_n'(x_2)], \end{aligned}$$

$$B_1 = x_3[A_2 x_1 j_n'(x_1) - A_1 j_n(x_2)],$$

$$\tan \eta_n = -\frac{[B_2 j_n'(x_3) - B_1 j_n(x_3)]}{[B_2 n_n'(x_3) - B_1 n_n(x_3)]},$$

where ρ_3 is the density of the water, c_3 is the sound speed in the water, a is the radius of the sphere, ρ_1 is the density of the sphere material, and c_1 and c_2 are the speeds of the longitudinal and transverse waves within the sphere, respectively (Table I). In the far field, at large range (r), or $k_3 r \gg 1$, the form function is

$$f(\theta) = \frac{1}{k_3} \sum_{n=0}^{\infty} (2n+1) \sin \eta_n \exp(i \eta_n) P_n(\cos \theta).$$

The total scattering cross section (σ_t) can be equivalently computed using three different methods: (1) a discrete integration of the form function, (2) an analytical integration of the Legendre polynomial, or (3) by application of the optical theorem (Feenberg, 1932). The discrete integration can be computed by

$$\sigma_t = \int_0^{2\pi} \int_0^{\pi} |f(\theta)|^2 d \cos \theta \, d\varphi$$

$$= -2\pi \int_0^{\pi} \sin \theta |f(\theta)|^2 \, d\theta.$$

Analytical integration of the Legendre polynomials is

$$\sigma_t = \int |f|^2 d\Omega = \int_0^{2\pi} \int_0^{\pi} \left[\sum_n \frac{1}{k_3} (2n+1) \sin \eta_n \times \exp(i \eta_n) P_n(\cos \theta) \right] \times \left[\sum_m \frac{1}{k_3} (2m+1) \sin \eta_m \times \exp(i \eta_m) P_m(\cos \theta) \right] d \cos \theta d\varphi$$

$$\sigma_t = \frac{2\pi}{k_3^2} \sum_{nm} \sin \eta_n \sin \eta_m \exp(i(\eta_n - \eta_m))(2n+1)(2m+1) \times \int_0^{\pi} P_n(\cos \theta) P_m(\cos \theta) d \cos \theta,$$

$$\sigma_t = \frac{2\pi}{k_3^2} \sum_n \sin^2 \eta_n \exp(i(\eta_n - \eta_n))(2n+1)^2 \frac{2}{2n+1},$$

$$\sigma_t = \frac{4\pi}{k_3^2} \sum_{n=0}^{\infty} (2n+1) \sin^2 \eta_n .$$

Finally, the conventional optical theorem involves the imaginary part (Im) of the forward-scattering form function:

$$\sigma_t = \frac{4\pi}{k_3} \mathrm{Im}(f(0)).$$

Applied to elastic spheres, the total scattering cross section is efficiently derived by

$$\sigma_t = \frac{4\pi}{k_3^2} \sum_{n=0}^{\infty} (2n+1) \sin \eta_n \, \mathrm{Im}(\exp(i \eta_n)).$$

Conti, S. G., and Demer, D. A. (**submitted**). "Wide-bandwidth acoustical characterization of anchovy and sardine from reverberation measurements in an echoic tank," ICES J. Mar. Sci.

Demer, D. A., and Conti, S. G. (**submitted**). "Broadbandwidth total target strength measurements of Antarctic krill (*Euphausia superba*) from reverberation in a cavity," ICES J. Mar. Sci.

Demer, D. A., and Conti, S. G. (**in press**). "Reconciling theoretical versus empirical target strengths of krill; effects of phase variability on the distorted wave Born approximation," ICES J. Mar. Sci.

Demer, D. A., Soule, M. A., and Hewitt, R. P. (**1999**). "A multiple-frequency method for potentially improving the accuracy and precision of *in situ* target strength measurements," J. Acoust. Soc. Am. **105**(4), 2359–2376.

De Rosny, J. (**2000**). "Milieux réverbérants et réversibilité," Thèse de Doctorat Université Paris VI.

De Rosny, J., and Roux, P. (**2001**). "Multiple scattering in a reflecting cavity: Application to fish counting in a tank," J. Acoust. Soc. Am. **109**, 2587–2597.

Diachok, O., Liorzou, B., and Scalabrin, C. (**2001**). "Estimation of the number density of fish from resonance absorptivity and echo sounder data," ICES J. Mar. Sci. **58**, 137–153.

Ehrenberg, J. E., and Lytle, D. W. (**1972**). "Acoustic Techniques for Estimating Fish Abundance," IEEE Trans. Geosci. Electron. **GE-10**, 138–145.

Faran, J. J. (**1951**). "Sound scattering by solid cylinders and spheres," J. Acoust. Soc. Am. **23**, 405–418.

Feenberg, E. (**1932**). "The Scattering of Slow Electrons by Neutral Atoms," Phys. Rev. **40**(1), 40–54.

Foote, K. G. (**1982**). "Optimizing copper spheres for precision calibration of hydroacoustic equipment," J. Acoust. Soc. Am. **71**, 742–747.

Foote, K. G. (**1990**). "Spheres for calibrating an eleven-frequency acoustic measurement system," J. Cons., Cons. Int. Explor. Mer **46**, 284–286.

Foote, K. G., and MacLennan, D. N. (**1984**). "Comparison of copper and tungsten carbide calibration spheres," J. Acoust. Soc. Am. **75**, 612–616.

Hickling, R. (**1962**). "Analysis of echoes from a solid elastic sphere in water," J. Acoust. Soc. Am. **34**, 1582–1592.

Hickling, R. (**1964**). "Analysis of echoes from a hollow metallic sphere in water," J. Acoust. Soc. Am. **36**, 1124–1137.

Love, R. H. (**1977**). "Target strength of an individual fish at any aspect," J. Acoust. Soc. Am. **62**, 1397–1403.

Lubbers, J., and Graaf, R. (**1998**). "A simple and accurate formula for the sound velocity in water," Ultrasound Med. Biol. **24**(7), 1065–1068.

MacLennan, D. N. (**1981**). "The theory of solid spheres as sonar calibration targets," Scottish Fisheries Research Report, No. 22.

MacLennan, D. N., and Dunn, J. R. (**1984**). "Estimation of sound velocities from resonance measurements on tungsten carbide calibration spheres," J. Sound Vib. **97**, 321–331.

McGehee, D. E., O'Driscoll, R. L., and Martin-Traykovski, L. V. (**1998**). "Effects of orientation on acoustic scattering from Antarctic krill at 120 kHz," Deep-Sea Res., Part II **45**, 1273–1294.

Weston, D. E. (**1967**). "Sound propagation in the presence of bladder fish," in *Underwater Acoustics*, edited by V. M. Albers (Plenum, New York), Vol. 2, pp. 55–88.